

## ELECTRONIC SUPORTING INFORMATION

# **Pd<sup>II</sup>/Ag<sup>I</sup> Catalyzed room temperature Reaction of $\gamma$ -Hydroxy Lactams: Mechanism, Scope, and antistaphylococcal activity**

Manali Dutta,<sup>a</sup> Santi M. Mandal,<sup>b</sup> Rupa Pegu,<sup>a</sup> and Sanjay Pratihar<sup>a,\*</sup>

Department of Chemical Sciences, Tezpur University, Napaam, Tezpur, Assam, India, 784028

Email: [spratihar@tezu.ernet.in](mailto:spratihar@tezu.ernet.in) or [spratihar29@gmail.com](mailto:spratihar29@gmail.com)

### Table of content:

Figure/Table Name	Page No.
Screening of solvent for $\alpha$ -amidoalkylation reaction	S2
ORTEP diagram of compound <b>2f</b>	S2
ORTEP diagram of compound <b>1c</b>	S3
Crystal data parameter for compound <b>1c</b> and <b>2f</b>	S4
Antimicrobial Study of the phthalimide derivatives	S5
<sup>1</sup> H and <sup>13</sup> C NMR of all the synthesised compounds	S6-S28
HRMS spectrum of selected compounds	S29-S32

**Table S1. Screening of solvent for  $\alpha$ -amidoalkylation reaction**

#	Solvent	T, °C	t, h	Yield, %
2	DCE	Rt	4	92
3	Toluene	Rt	6	56
4	DMF	Rt	6	0
5	MeCN	rt	4	<10
6	DCM	rt	4	82
7	THF	rt	6	32

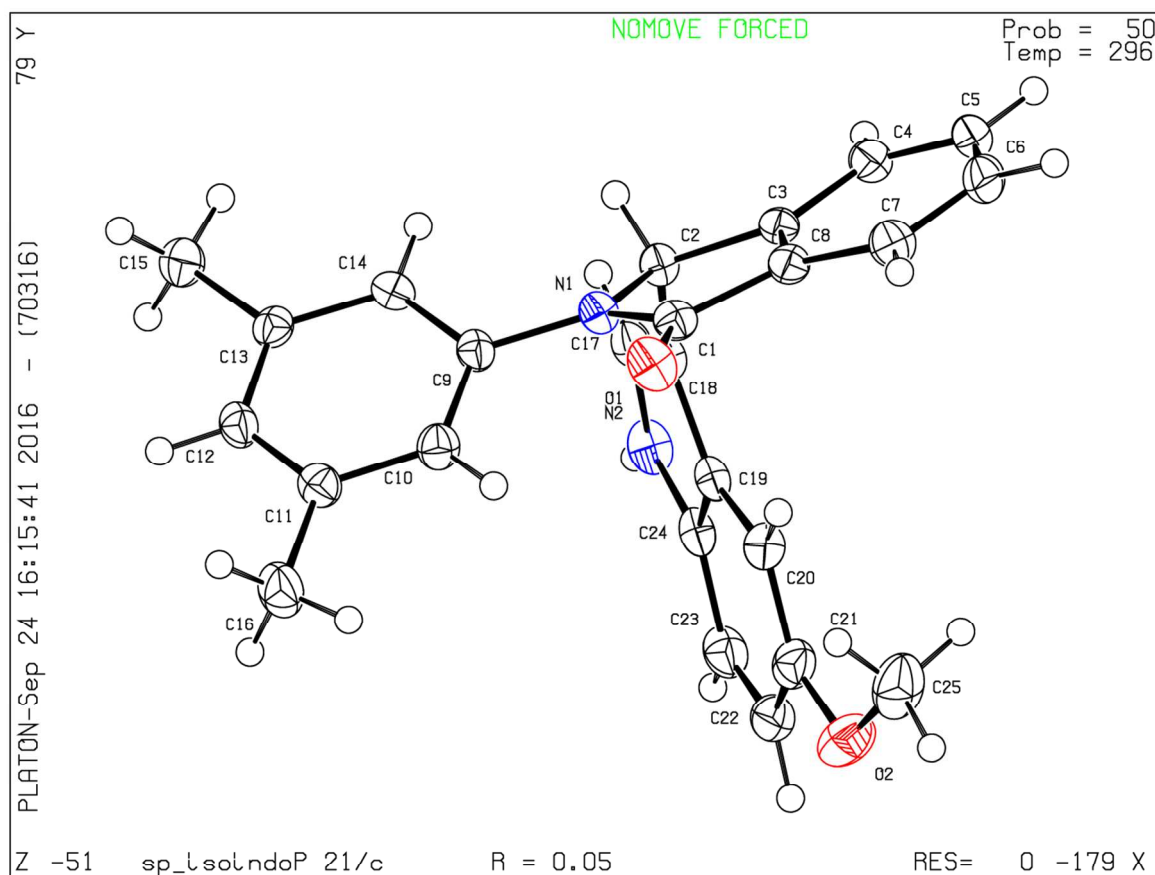


**Figure S1. ORTEP diagram of compound 2f.**

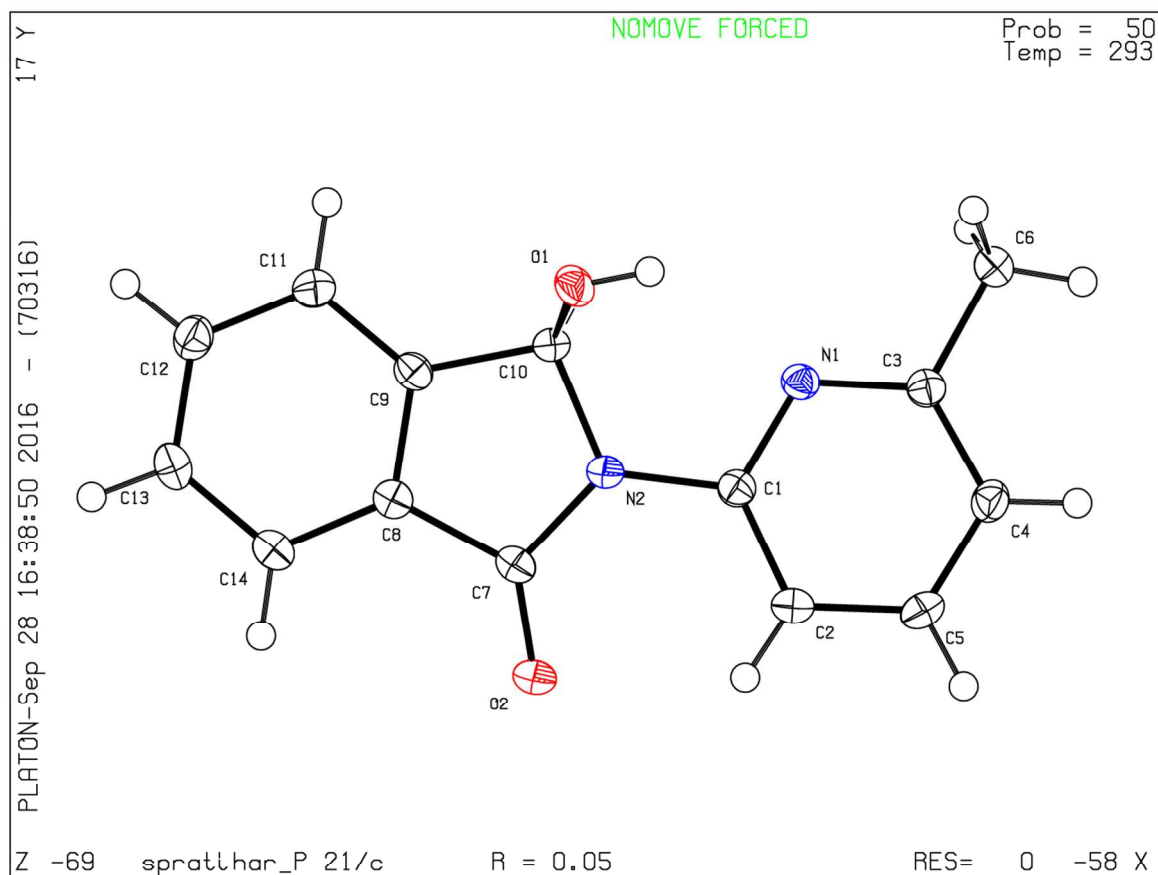


**Figure S2.** ORTEP diagram of compound **1c**.

**Table S2.** Crystal data parameter for compound **1c** and **2f**.

	<b>1c</b>	<b>2f</b>
Formula unit	C <sub>25</sub> H <sub>22</sub> O <sub>2</sub> N <sub>2</sub>	C <sub>25</sub> H <sub>22</sub> O <sub>2</sub> N <sub>2</sub>
Formula wt.	280.35	382.45
Crystal system	Monoclinic	Monoclinic
T [K]	296	296
<i>a</i> [Å]	6.9266(2)	9.2359(2)
<i>b</i> [Å]	14.6572(5)	14.0859(4)
<i>c</i> [Å]	11.4985(3)	15.6450(4)
$\alpha$ [°]	90	90
$\beta$ [°]	103.475(2)	101.897(2)
$\gamma$ [°]	90	90
Volume [Å <sup>3</sup> ]	1135.24(6)	1991.63(9)
Space group	<i>P</i> 2 <sub>1</sub> / <i>c</i>	<i>P</i> 2 <sub>1</sub> / <i>c</i>
<i>Z</i>	4	4
<i>D</i> <sub>calc</sub> [g cm <sup>-3</sup> ]	1.406	1.276
$\mu$ /mm <sup>-1</sup>	0.096	0.081
Reflns. Collected	2609	4620
Unique reflns.	2320	3180
<i>R</i> <sub>1</sub> [ <i>I</i> >2 $\sigma$ ( <i>I</i> )], <i>wR</i> <sub>2</sub>	0.0466; 0.1450	0.0502; 0.1611
GOF	1.172	1.099
Instrument	Bruker APEX-II	Bruker APEX-II
X-ray	MoK $\alpha$ ; $\lambda$ =0.71073	MoK $\alpha$ ; $\lambda$ =0.71073
CCDC Reference No.	<b>1501922</b>	<b>1506191</b>

**Antimicrobial assay:** Compounds were tested for antimicrobial against three strains, one negative control strain (Methicillin susceptible strain), *S. aureus* ATCC25923; one positive control strain (Methicillin resistant strain), *S. aureus* ATCC43300 and one clinical isolate which is both methicillin and vancomycin resistant, *S. aureus* U07 (Am J Infect Control. 2015 Dec 1;43(12):e87-8). Minimum inhibitory concentration (MIC) values of all compounds were determined following CLSI guidelines (CLSI, 2007). Compounds were dissolved in DMSO and concentration of each compound for the assay ranged from 500  $\mu$ g.mL<sup>-1</sup> to 0.24  $\mu$ g.mL<sup>-1</sup>. MIC

values were determined where no visible growth was observed. The culture conditions and bacterial growth were monitored in Muller Hinton Broth at 37°C. Two rows of wells, ones in which no compounds were added as positive controls, and the ones in which only medium were used as negative controls in order to maintain the experimental sterility. All experiments were repeated three times.

<b>Table S3.</b> Effect of pthalimide derivatives on MRSA and VRSA positive strains			
<b>Compounds</b>	<i>S. aureus</i> U07 (VRSA+ & MRSA+)	<i>S. aureus</i> ATCC25923 (Control strain)	<i>S. aureus</i> ATCC43300 (MRSA+ Control)
<b>Vancomycin</b>	31.2	1.95	3.9
<b>Methicillin</b>	125	1.95	31.2
<b>Tetracycline</b>	500	3.9	500
<b>Gentamicin</b>	16	0.975	0.975
<b>Levofloxacin</b>	0.48	0.24	0.24
<b>2c</b>	15.6	7.8	15.6
<b>2d</b>	3.9	1.95	3.9
<b>2e</b>	1.95	0.975	0.975
<b>2f</b>	125	62.5	62.5
<b>2g</b>	>1000	>1000	>1000
<b>2h</b>	500	250	500
<b>2i</b>	>1000	>1000	>1000
<b>2j</b>	>1000	>1000	>1000
<b>2k</b>	15.6	7.8	15.6
<b>2l</b>	1.95	0.975	0.975
<b>2m</b>	>1000	>1000	>1000
<b>2n</b>	>1000	>1000	>1000
<b>2o</b>	>1000	>1000	>1000
<b>2p</b>	>1000	>1000	>1000
<b>2q</b>	>1000	>1000	>1000
<b>2r</b>	500	250	500
<b>2s</b>	>1000	>1000	>1000
<b>2t</b>	7.8	0.975	1.95
<b>2u</b>	>1000	>1000	>1000
<b>2v</b>	>1000	>1000	>1000
<b>2w</b>	0.487	0.487	0.487

**Figure S3.**  $^1\text{H}$  and  $^{13}\text{C}$  NMR of **2a** in  $\text{DMSO-d}_6$  at 298K.

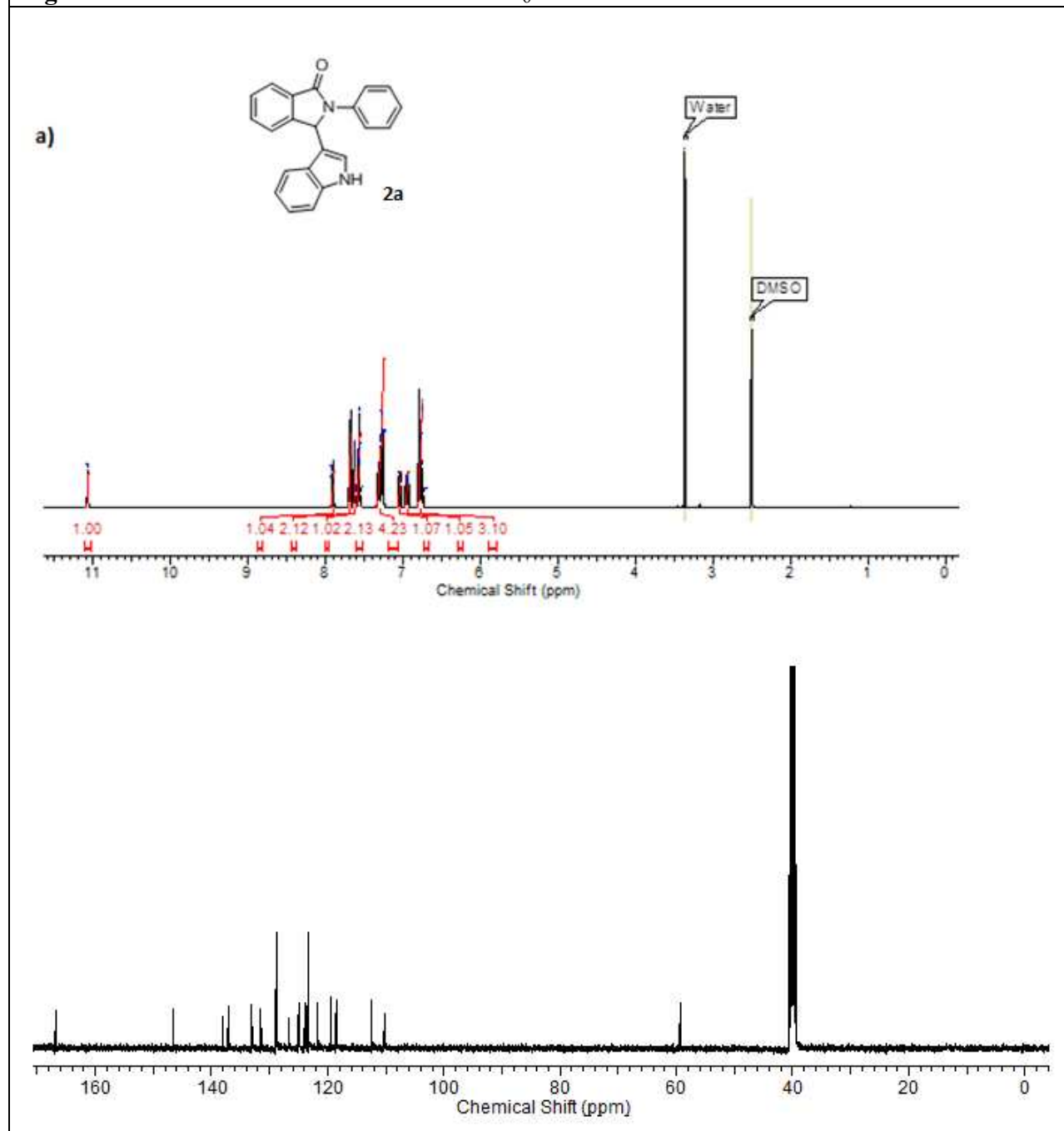


**Figure S4.**  $^1\text{H}$  and  $^{13}\text{C}$  NMR of **2b** in  $\text{DMSO-d}_6$  at 298K.

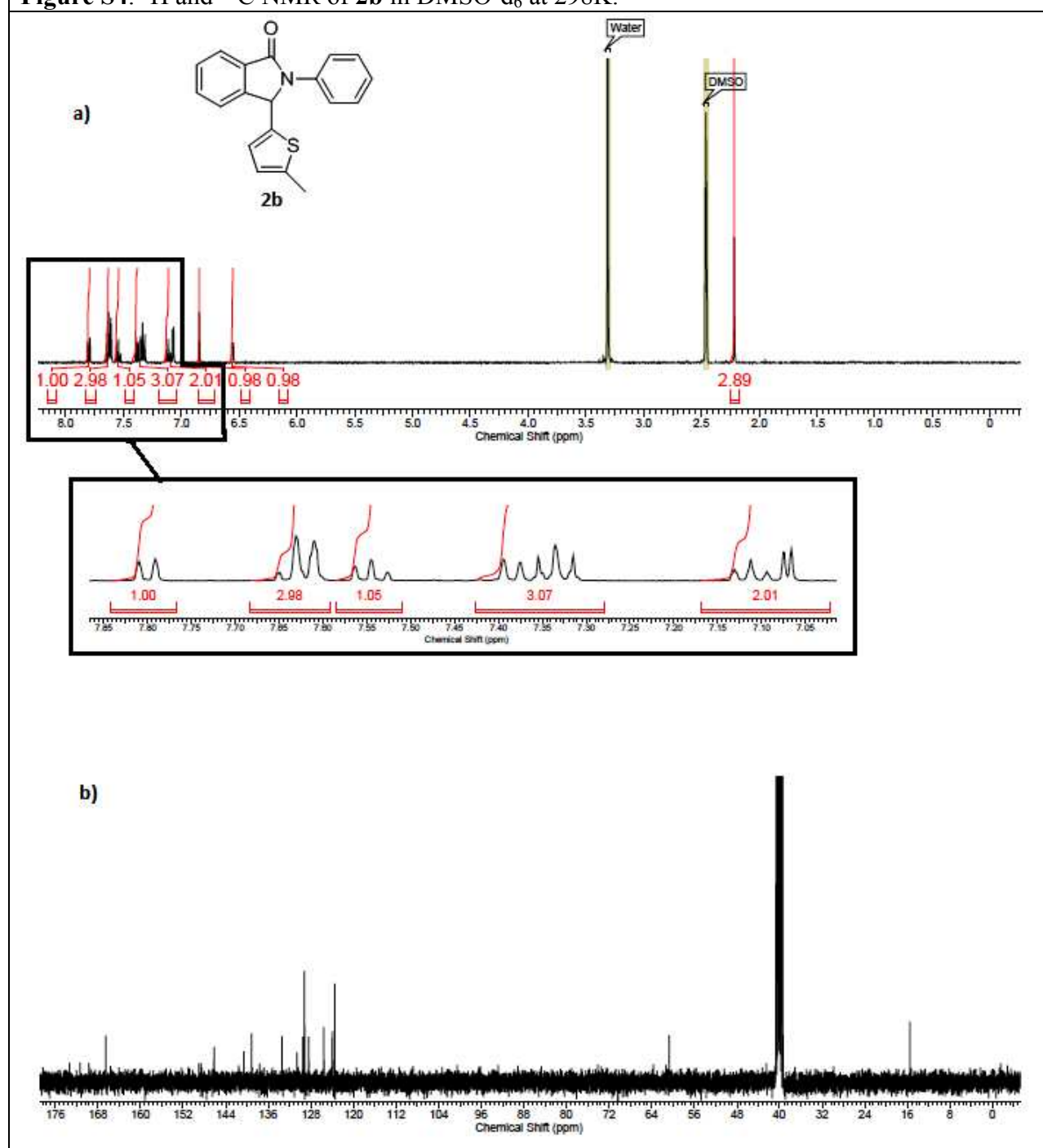


**Figure S5.**  $^1\text{H}$  and  $^{13}\text{C}$  NMR of **2c** in  $\text{DMSO-d}_6$  at 298K.

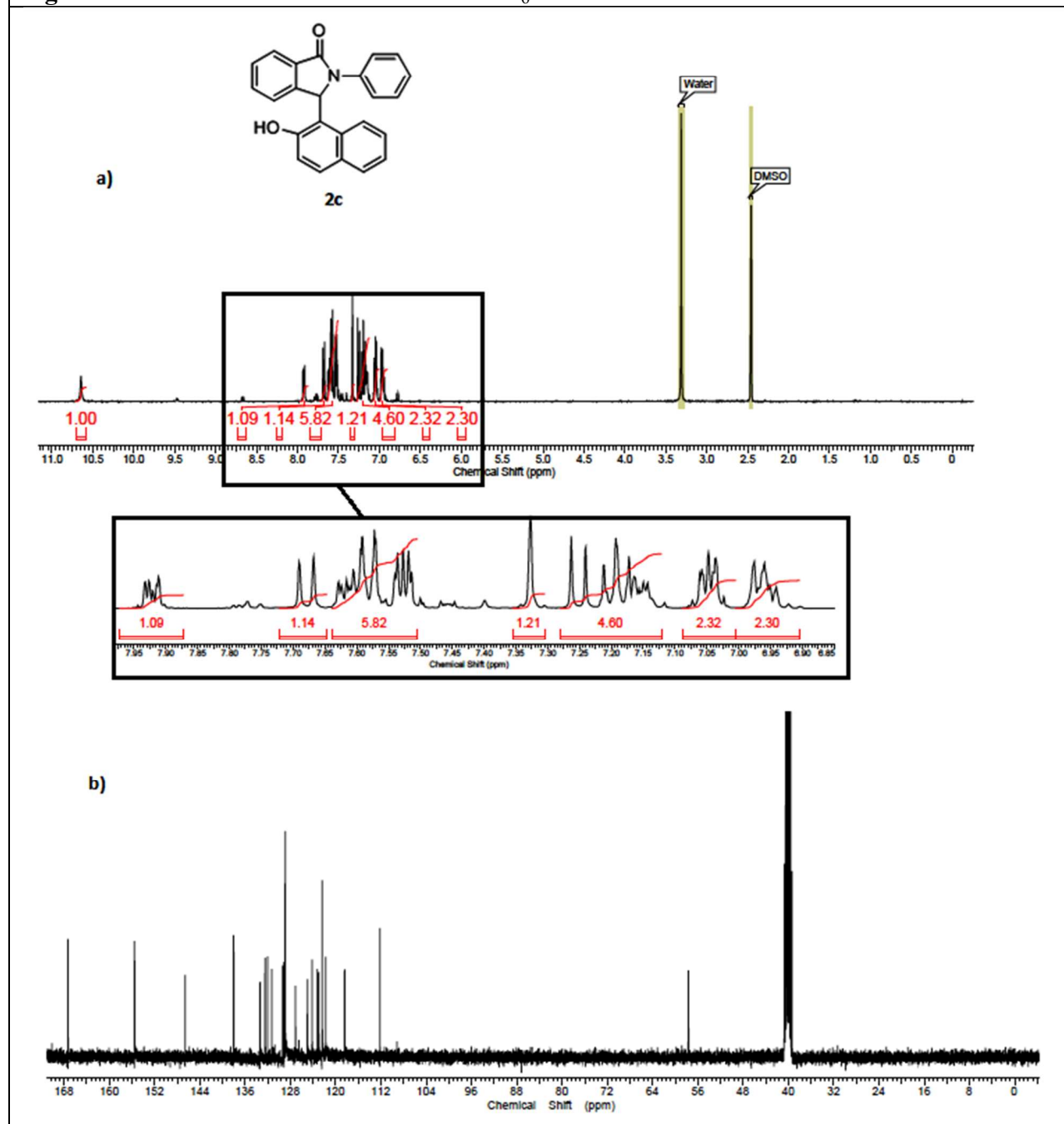


**Figure S6.**  $^1\text{H}$  and  $^{13}\text{C}$  NMR of **2d** in  $\text{DMSO-d}_6$  at 298K.

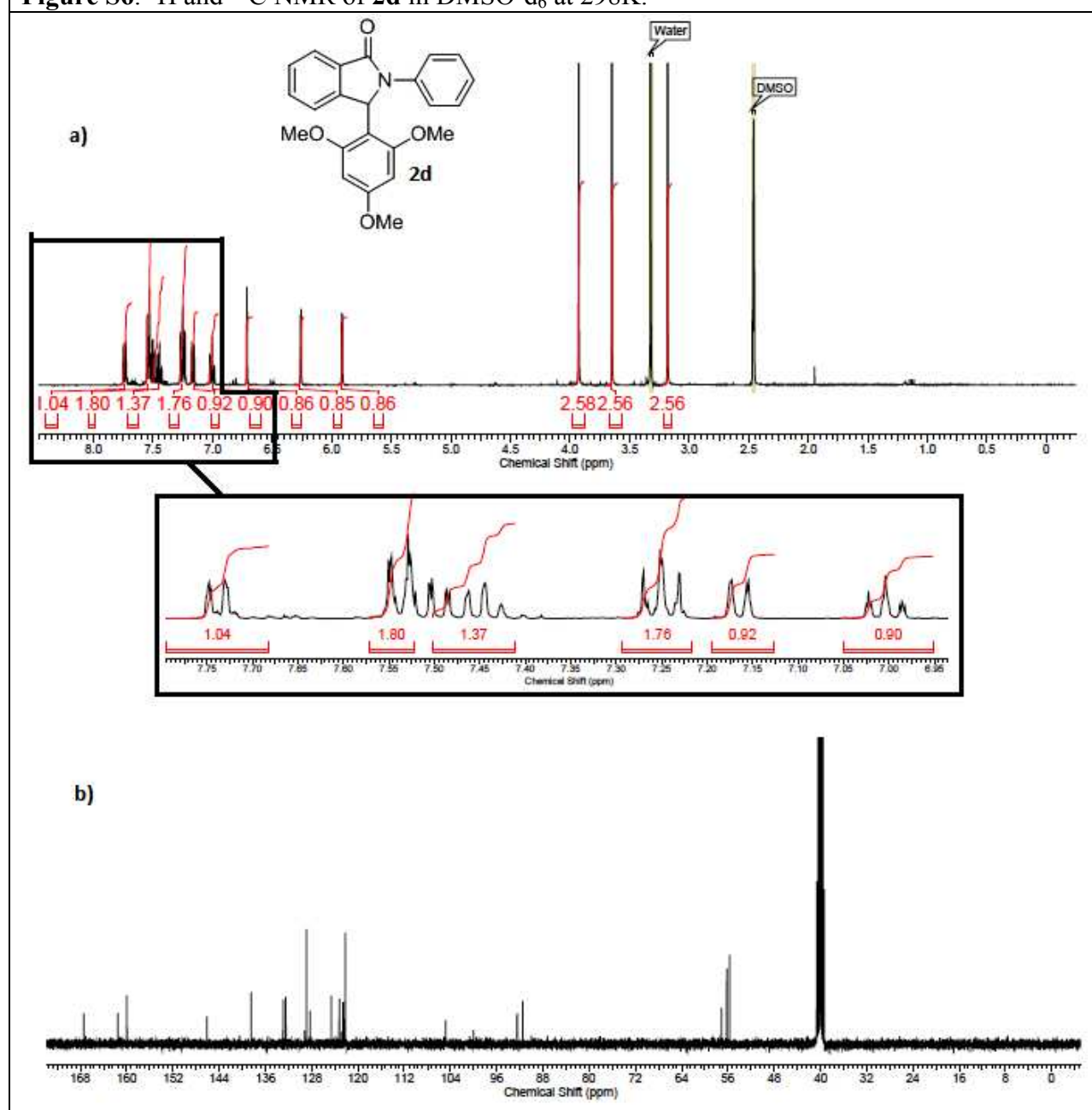


**Figure S7.**  $^1\text{H}$  and  $^{13}\text{C}$  NMR of **2e** in  $\text{DMSO-d}_6$  at 298K.

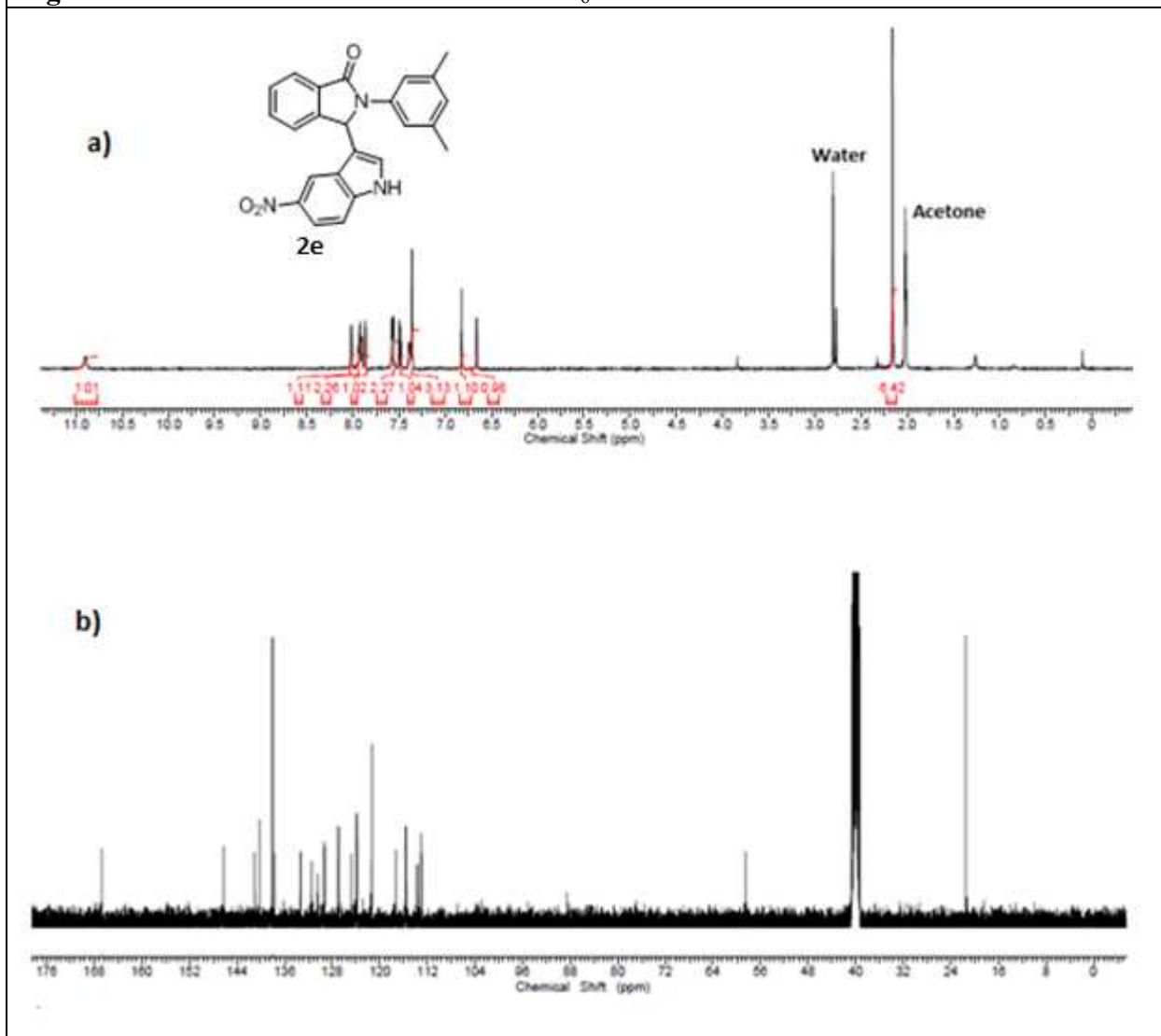


**Figure S8.**  $^1\text{H}$  and  $^{13}\text{C}$  NMR of **2f** in  $\text{DMSO-d}_6$  at 298K.

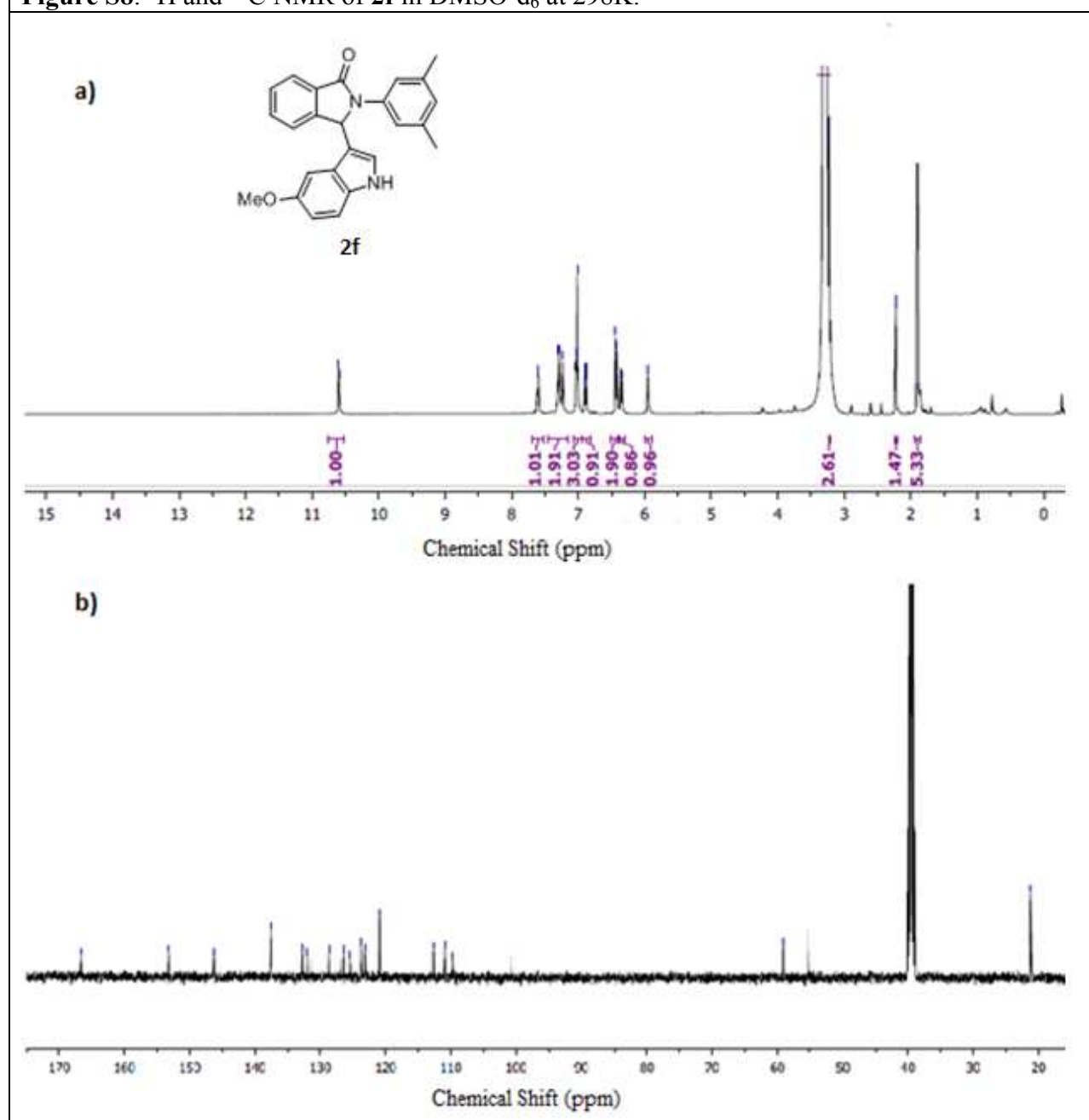


**Figure S9.**  $^1\text{H}$  and  $^{13}\text{C}$  NMR of **2g** in  $\text{DMSO-d}_6$  at 298K.

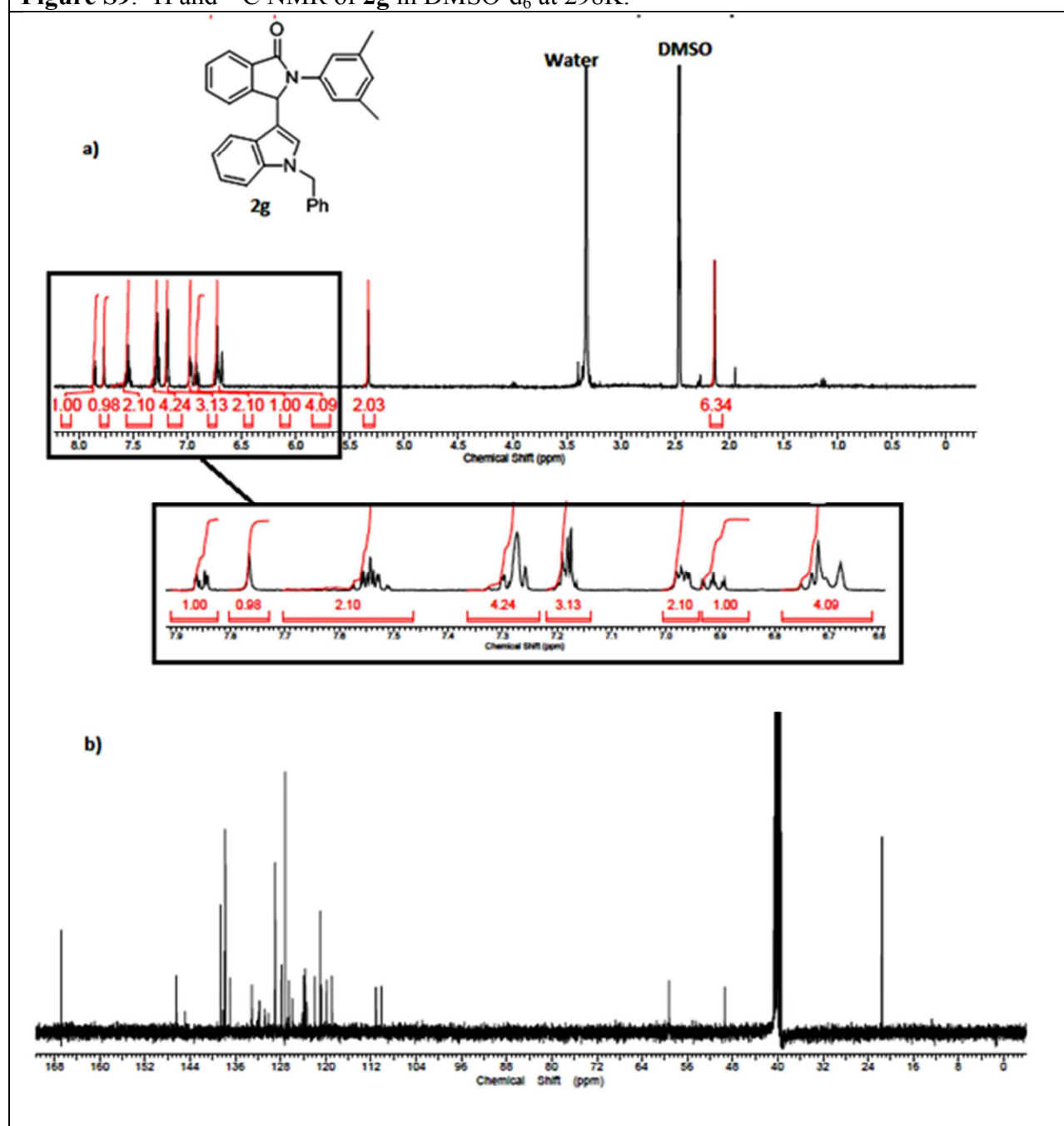


**Figure S10.**  $^1\text{H}$  and  $^{13}\text{C}$  NMR of **2h** in  $\text{CDCl}_3$  at 298K.

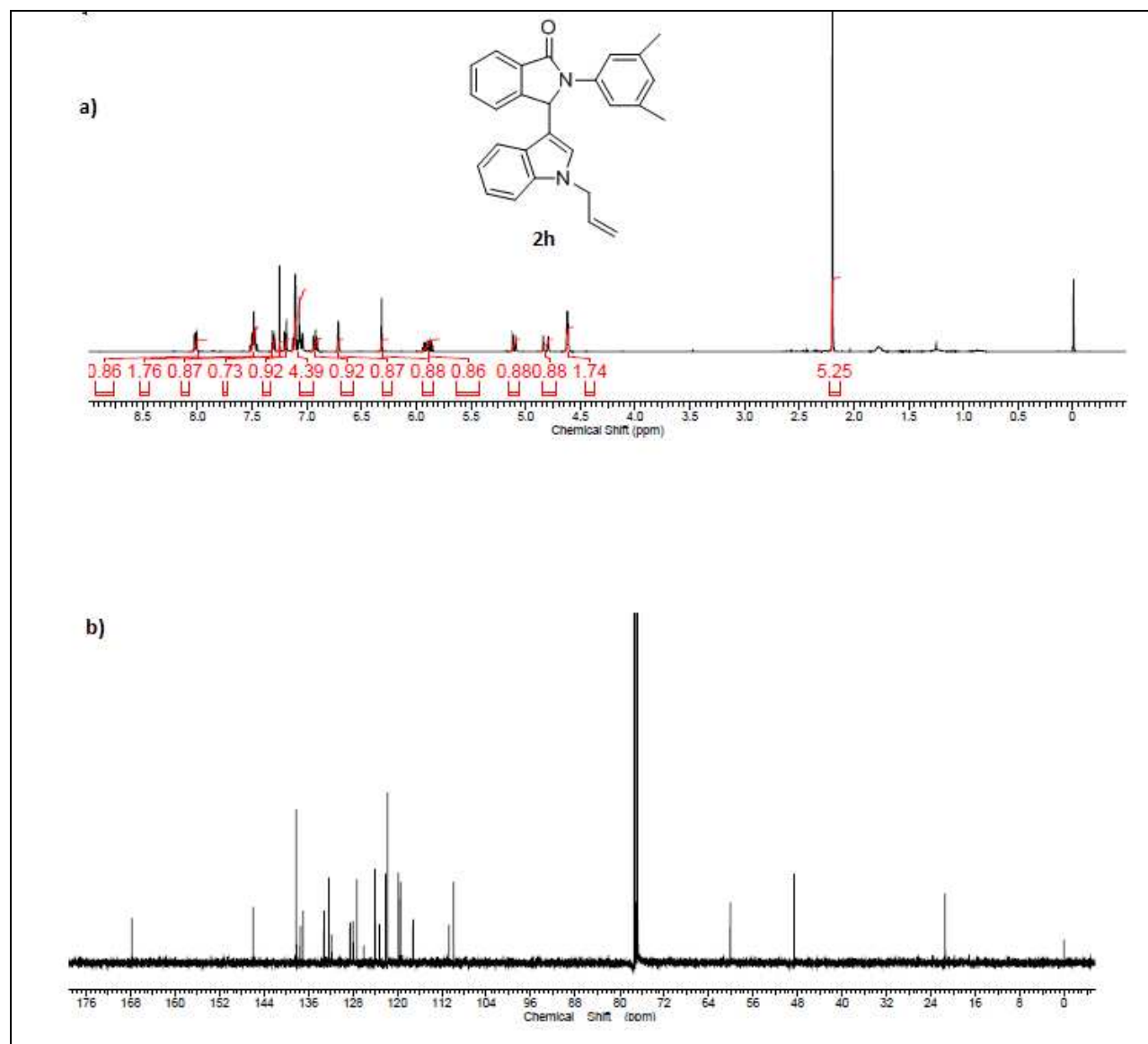


**Figure S11.**  $^1\text{H}$  and  $^{13}\text{C}$  NMR of **2i** in  $\text{CDCl}_3$  at 298K.

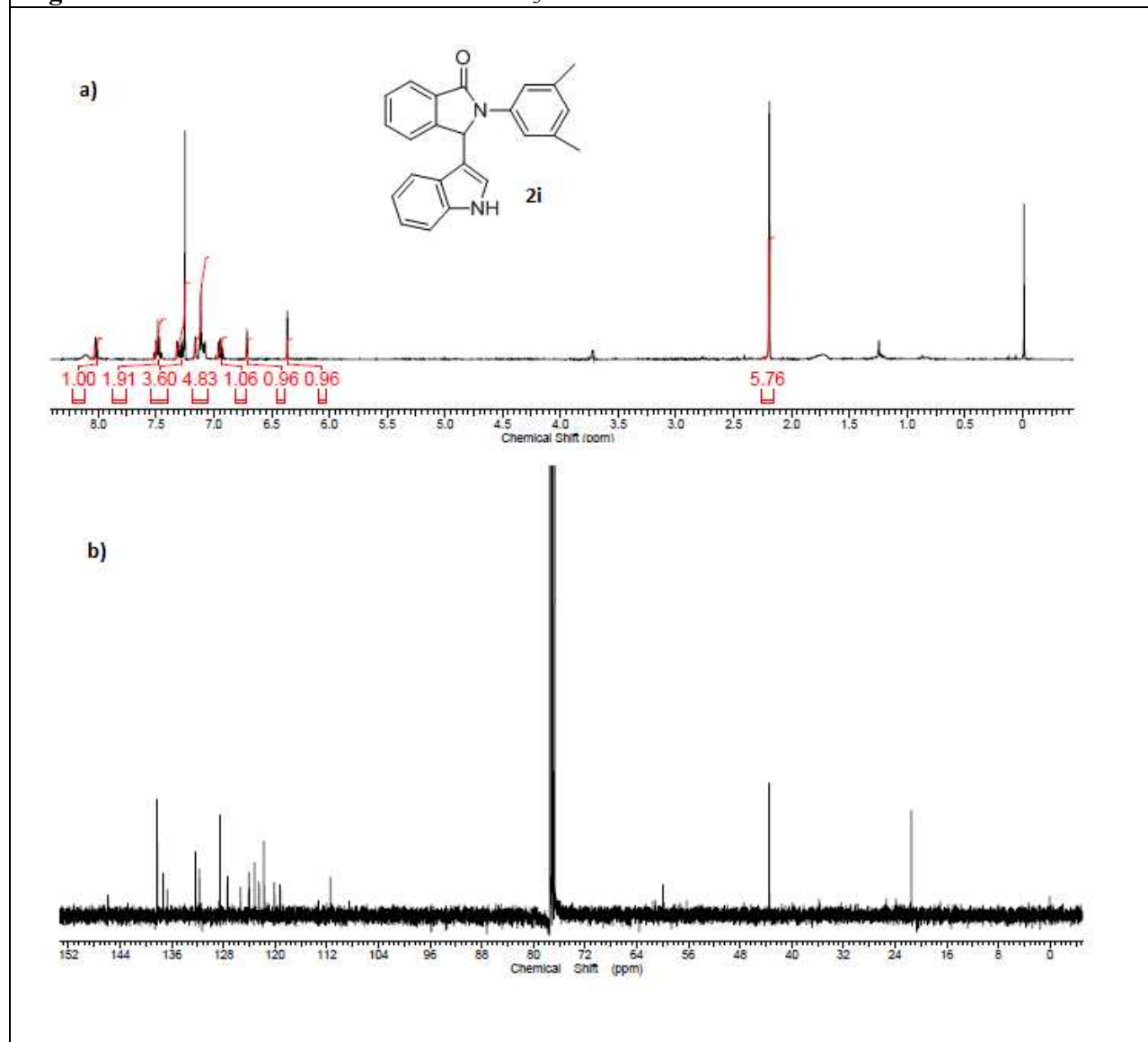


**Figure S12.**  $^1\text{H}$  and  $^{13}\text{C}$  NMR of **2j** in  $\text{CDCl}_3$  at 298K.

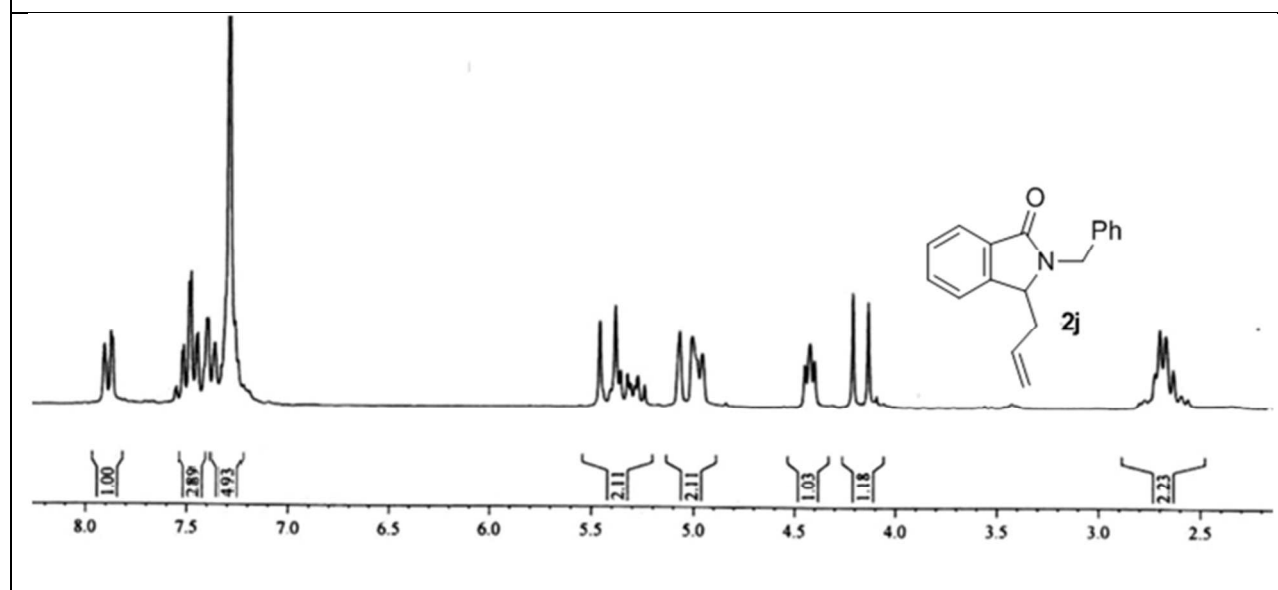


**Figure S13.**  $^1\text{H}$  and  $^{13}\text{C}$  NMR of **2k** in  $\text{DMSO-d}_6$  at 298K.

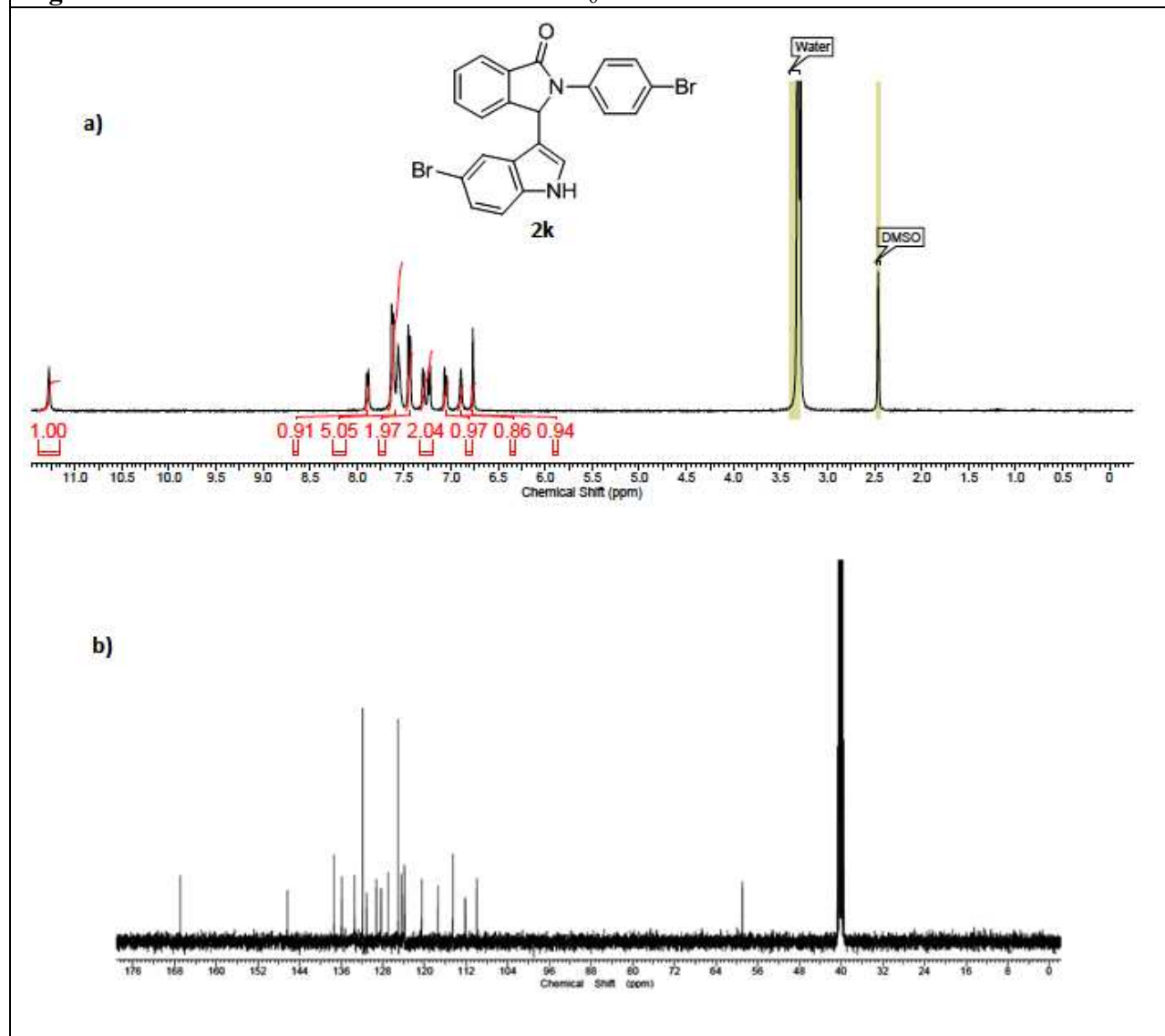


**Figure S14.**  $^1\text{H}$  and  $^{13}\text{C}$  NMR of **2l** in DMSO- $\text{d}_6$  at 298K.

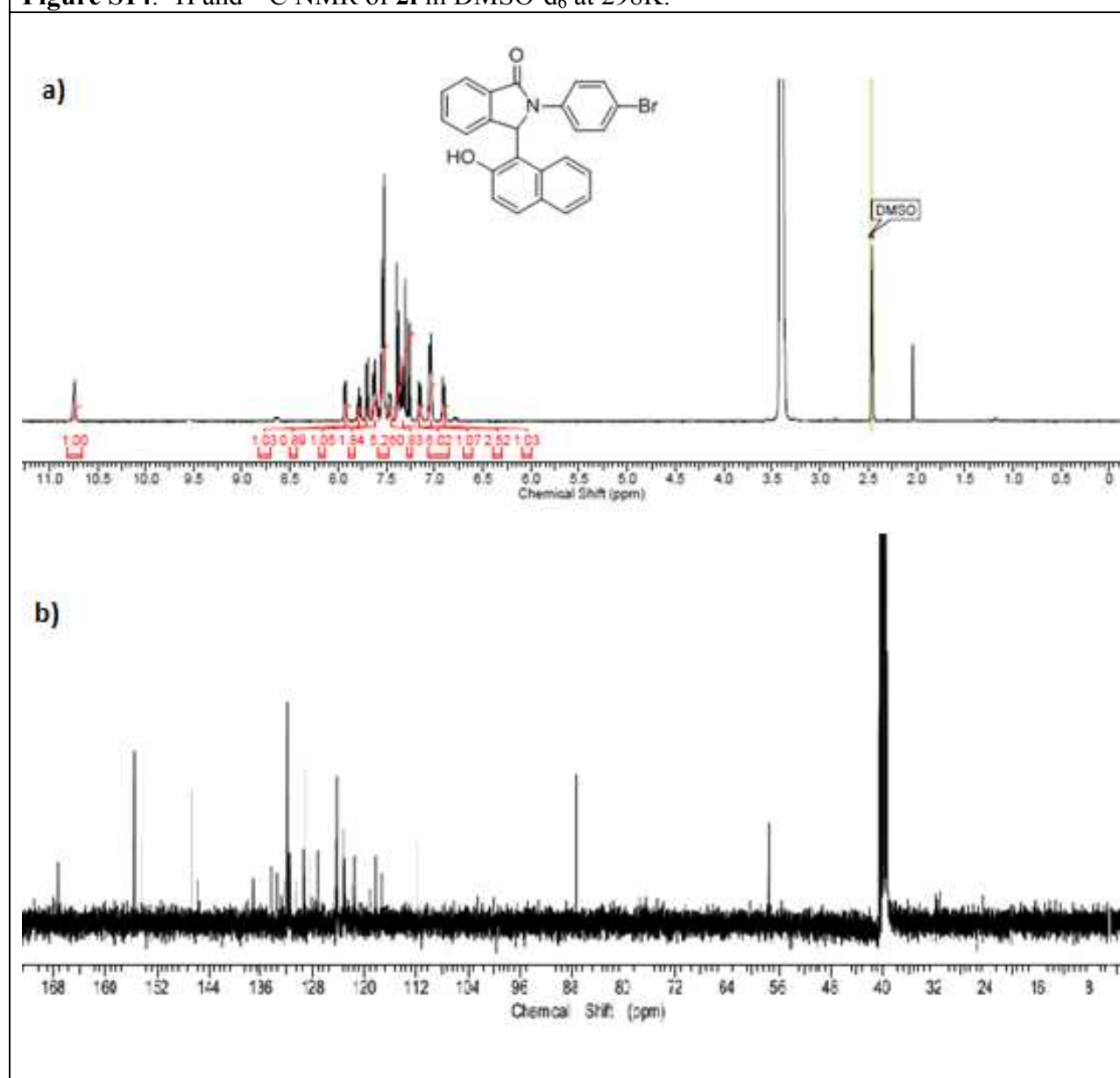


**Figure S15.**  $^1\text{H}$  and  $^{13}\text{C}$  NMR of **2m** in DMSO- $\text{d}_6$  at 298K.

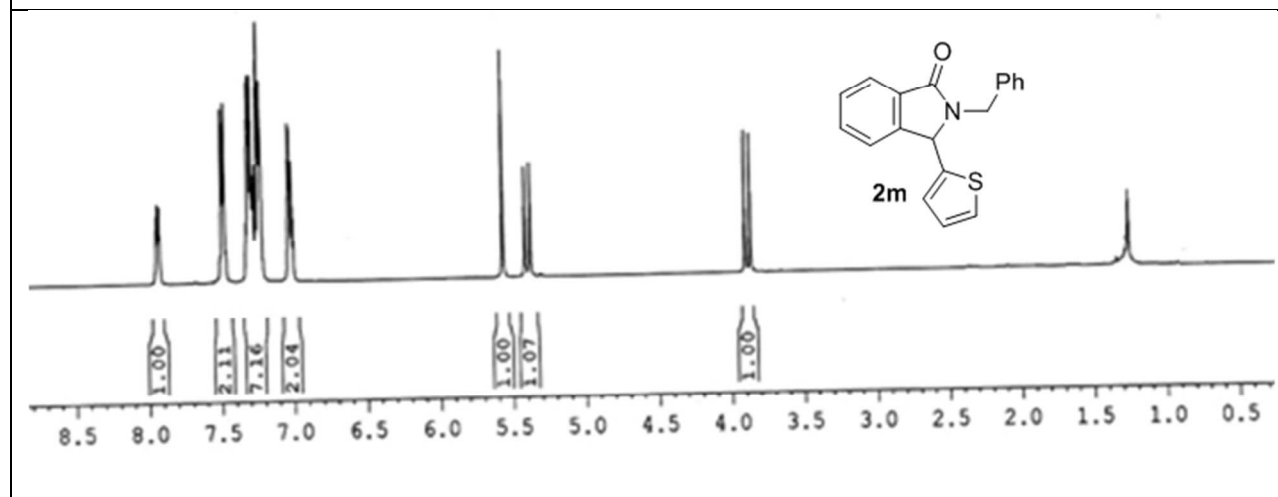


**Figure S16.**  $^1\text{H}$  and  $^{13}\text{C}$  NMR of **2n** in  $\text{DMSO-d}_6$  at 298K.

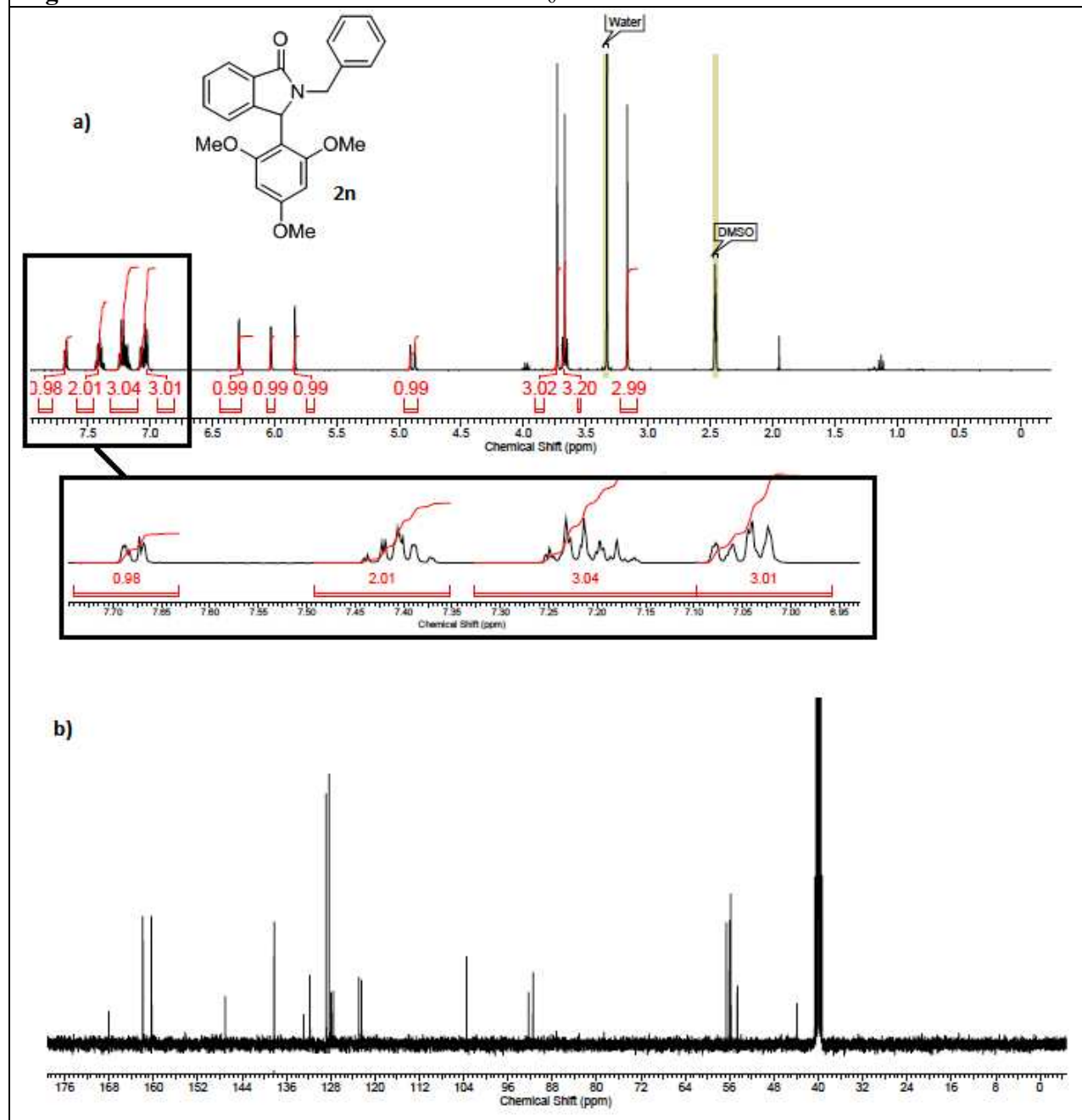


**Figure S17.**  $^1\text{H}$  and  $^{13}\text{C}$  NMR of **2o** in  $\text{CDCl}_3$  at 298K.

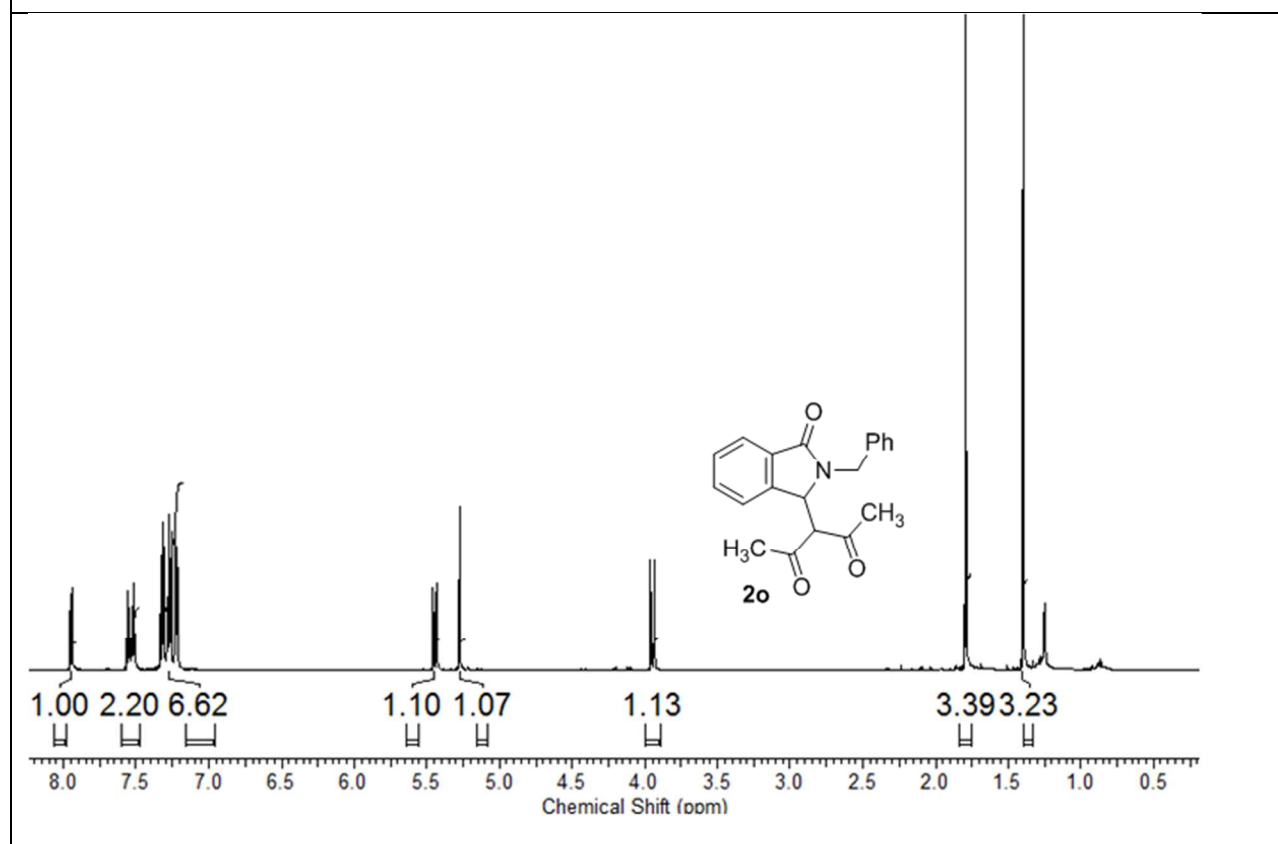


**Figure S18.**  $^1\text{H}$  and  $^{13}\text{C}$  NMR of **2p** in  $\text{CDCl}_3$  at 298K.

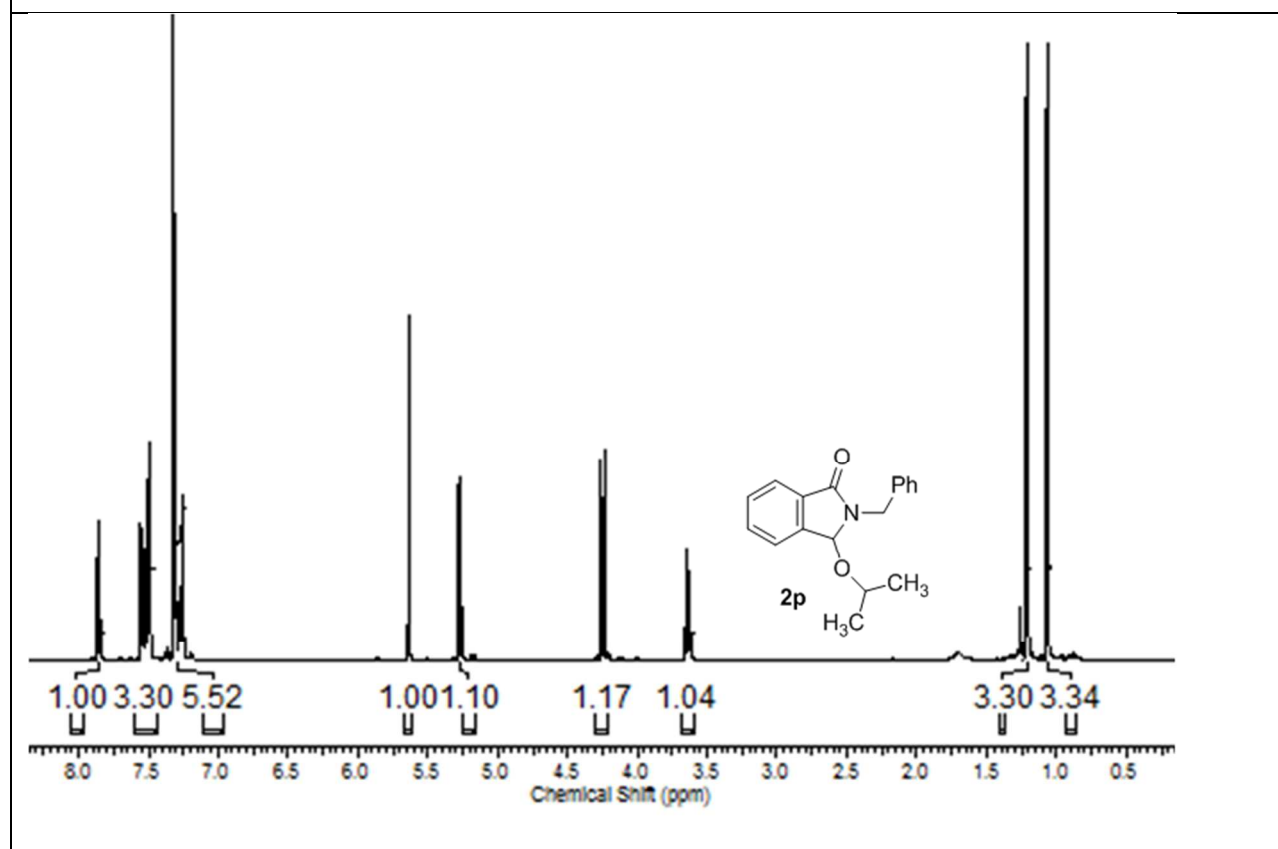


**Figure S19.**  $^1\text{H}$  and  $^{13}\text{C}$  NMR of **2q** in  $\text{CDCl}_3$  at 298K.

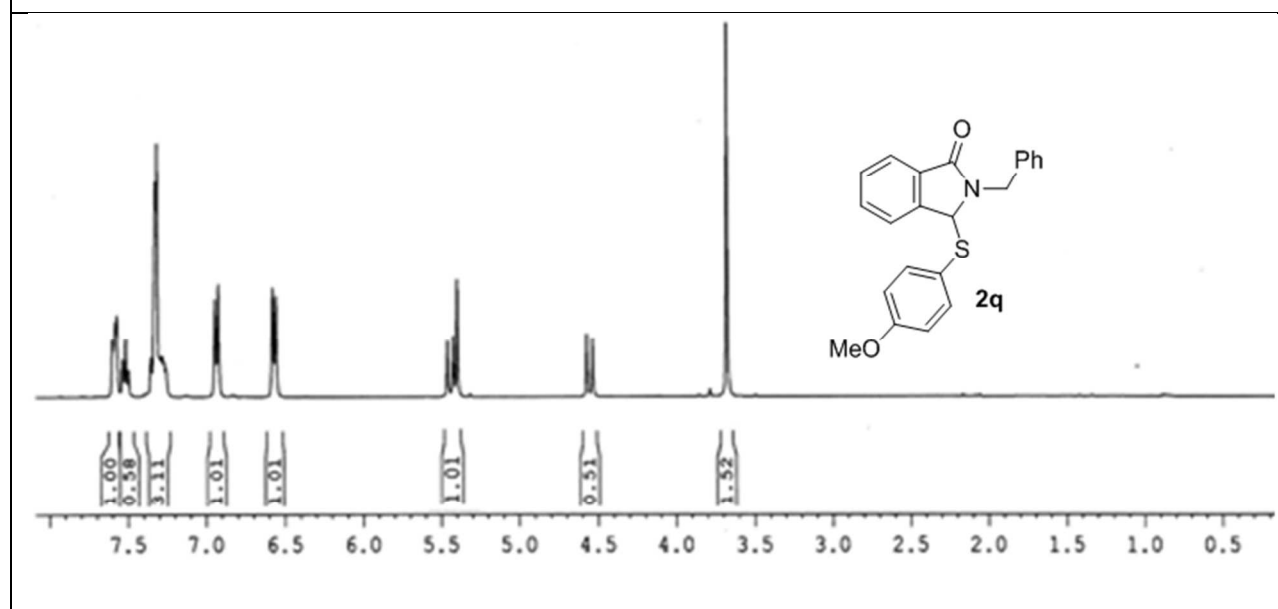


**Figure S20.**  $^1\text{H}$  and  $^{13}\text{C}$  NMR of **2r** in  $\text{DMSO-d}_6$  at 298K.

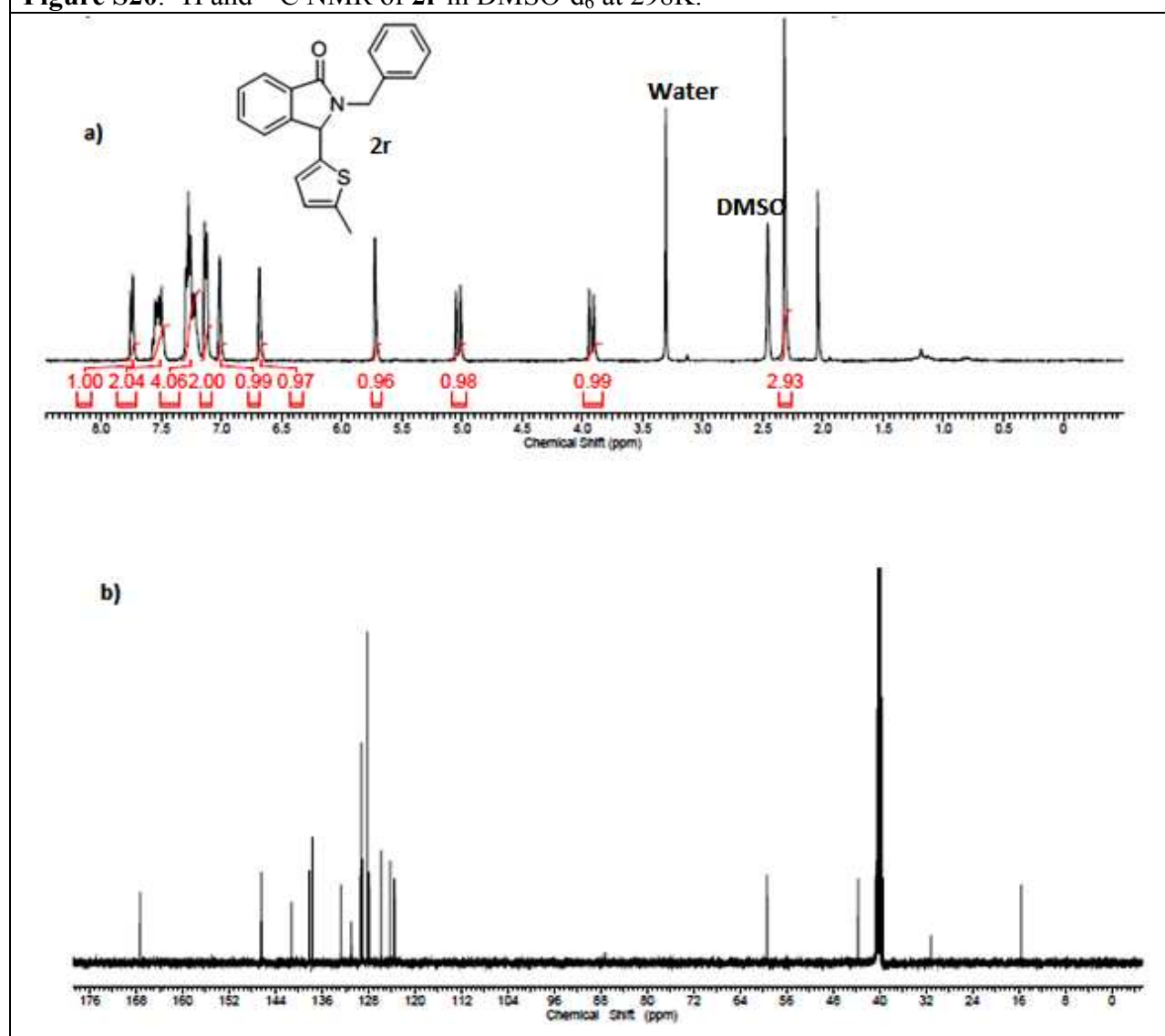


**Figure S21.**  $^1\text{H}$  and  $^{13}\text{C}$  NMR of **2s** in  $\text{DMSO-d}_6$  at 298K.

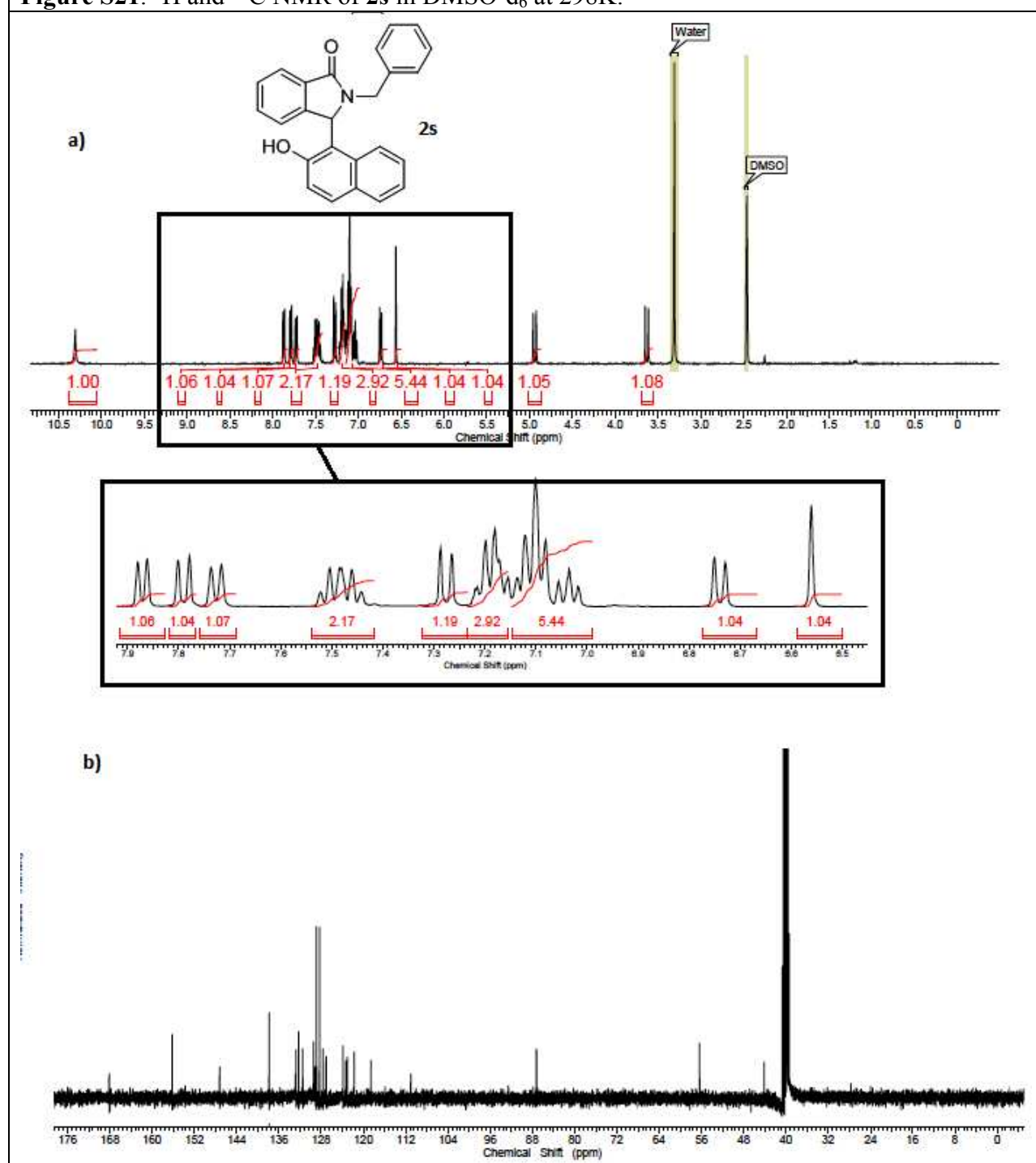


**Figure S22.**  $^1\text{H}$  and  $^{13}\text{C}$  NMR of **2t** in DMSO- $d_6$  at 298K.

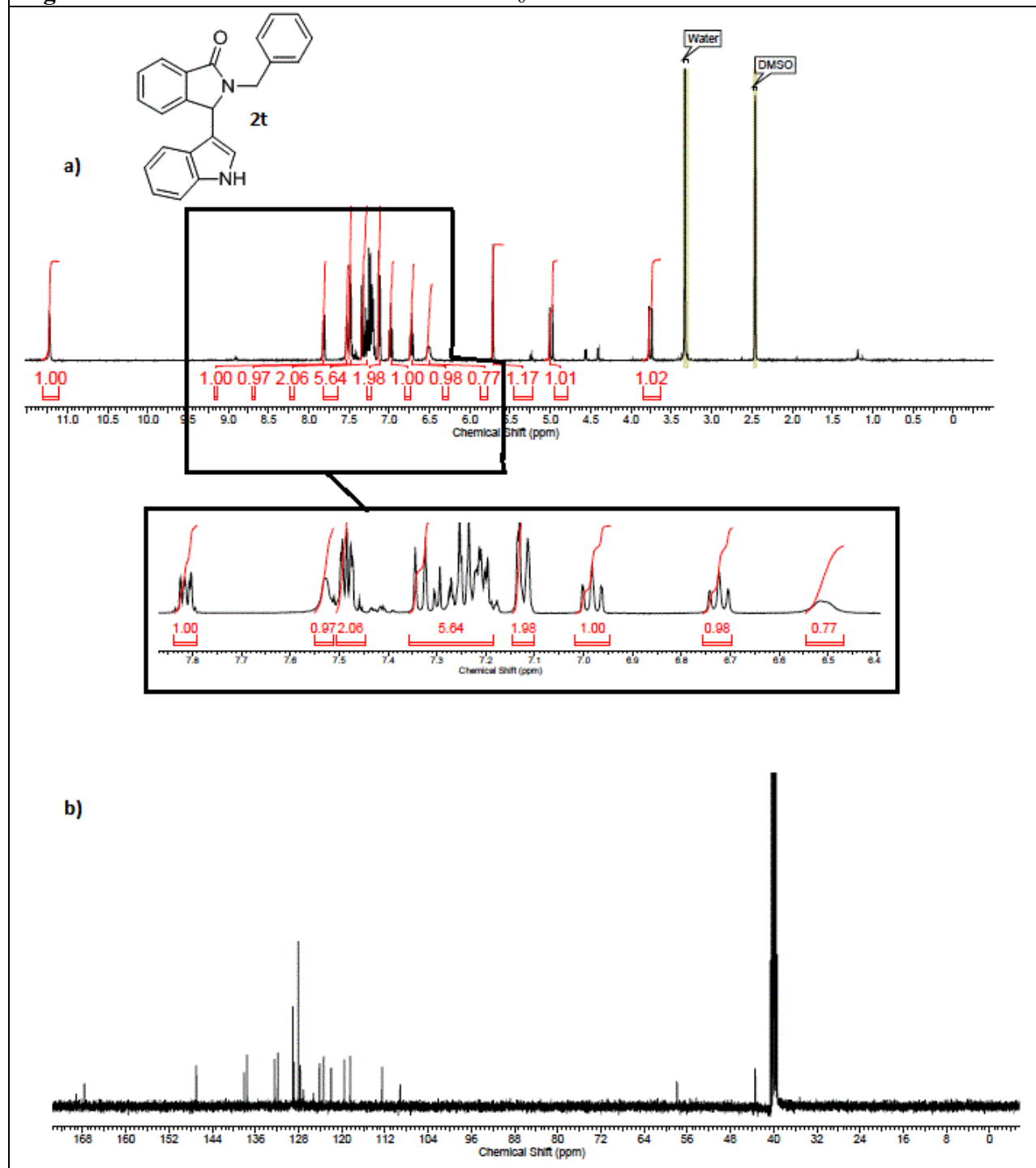


**Figure S23.**  $^1\text{H}$  and  $^{13}\text{C}$  NMR of **2u** in  $\text{DMSO-d}_6$  at 298K.

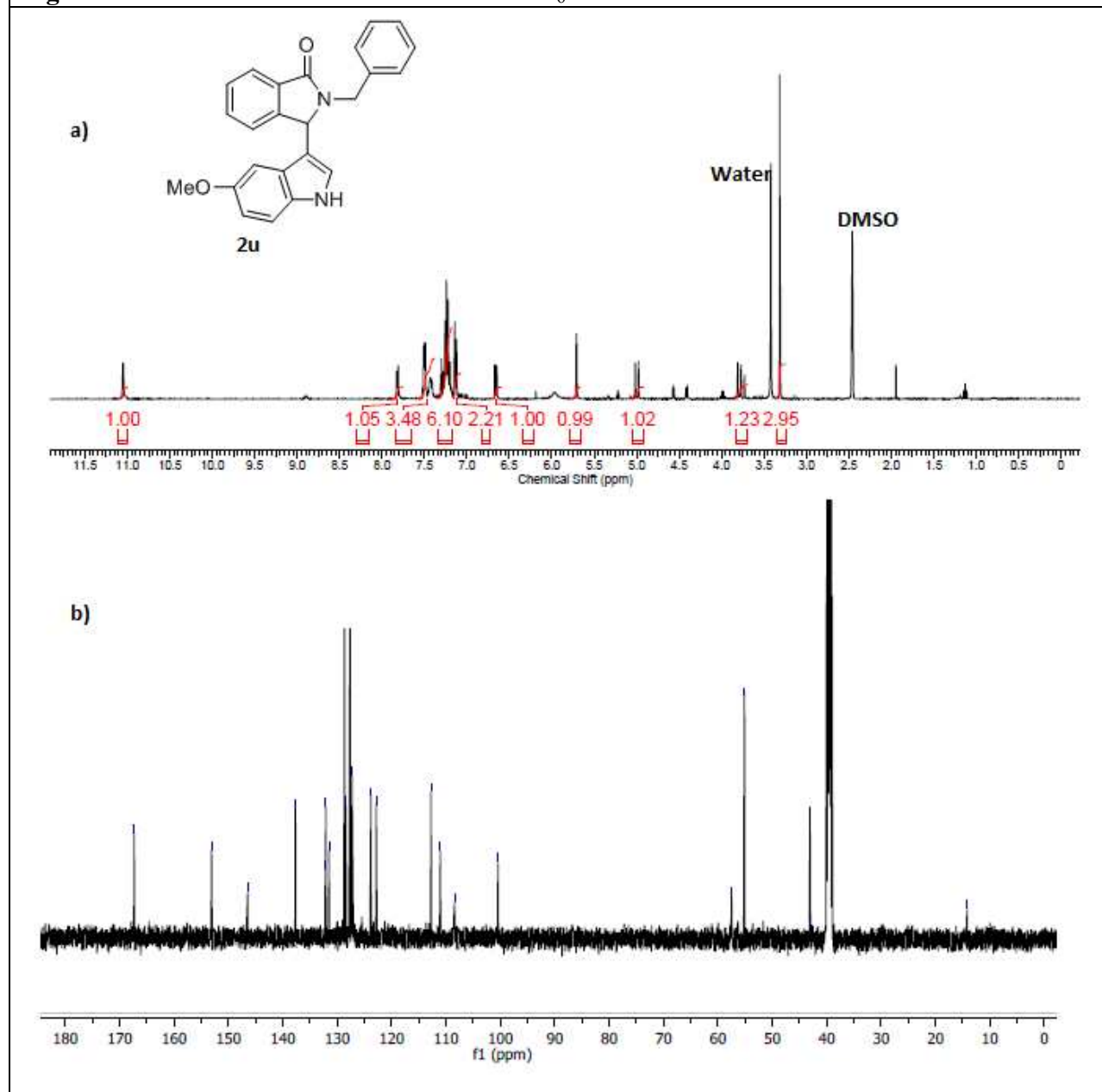


**Figure S24.**  $^1\text{H}$  and  $^{13}\text{C}$  NMR of **2v** in acetone- $\text{d}_6$  at 298K.

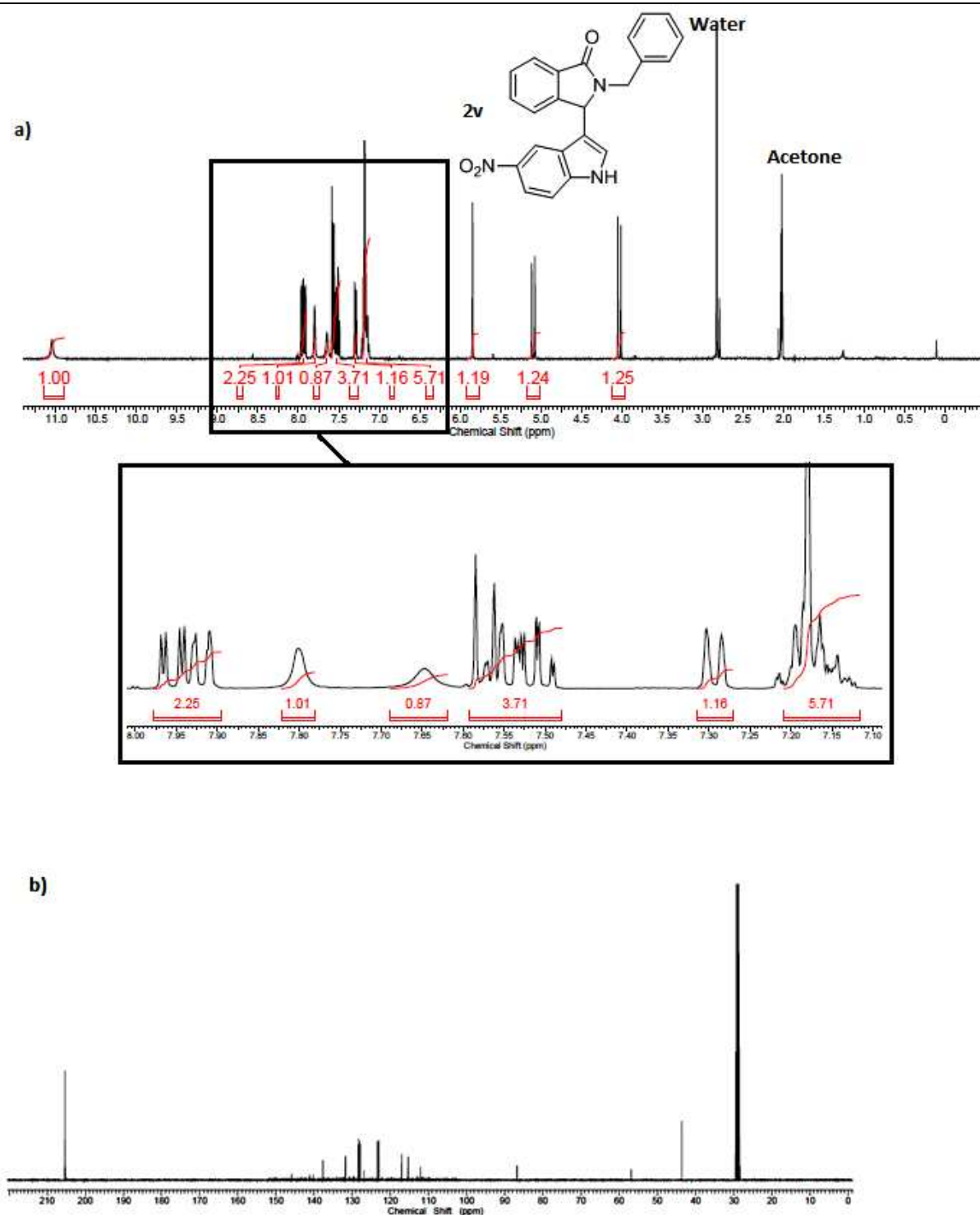


**Figure S25.**  $^1\text{H}$  and  $^{13}\text{C}$  NMR of **2w** in acetone- $\text{d}_6$  at 298K.

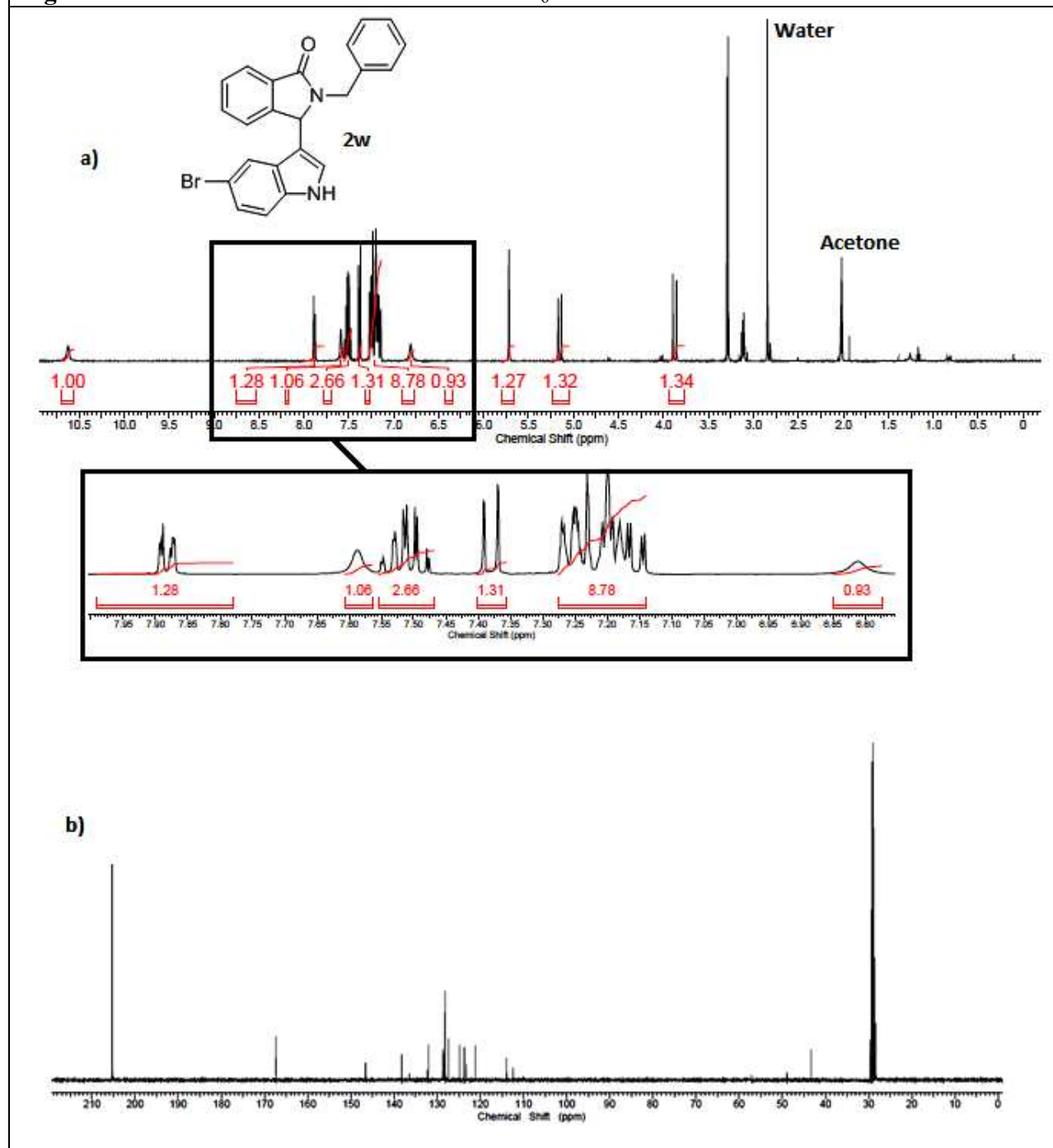
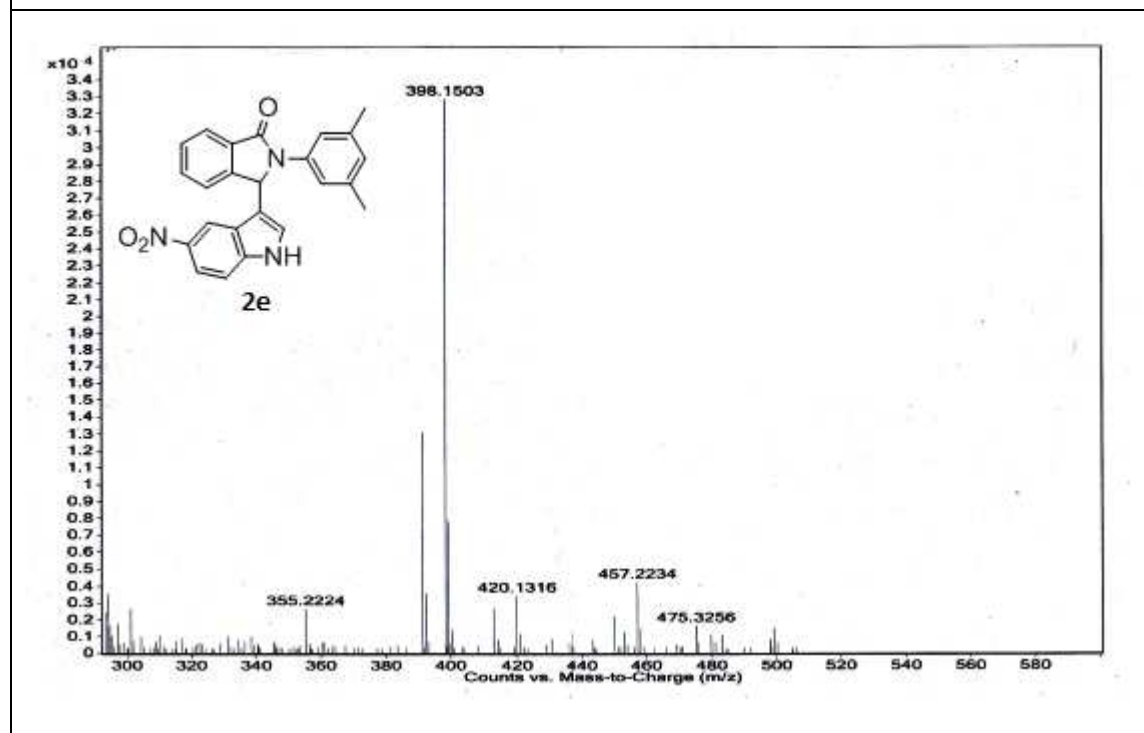
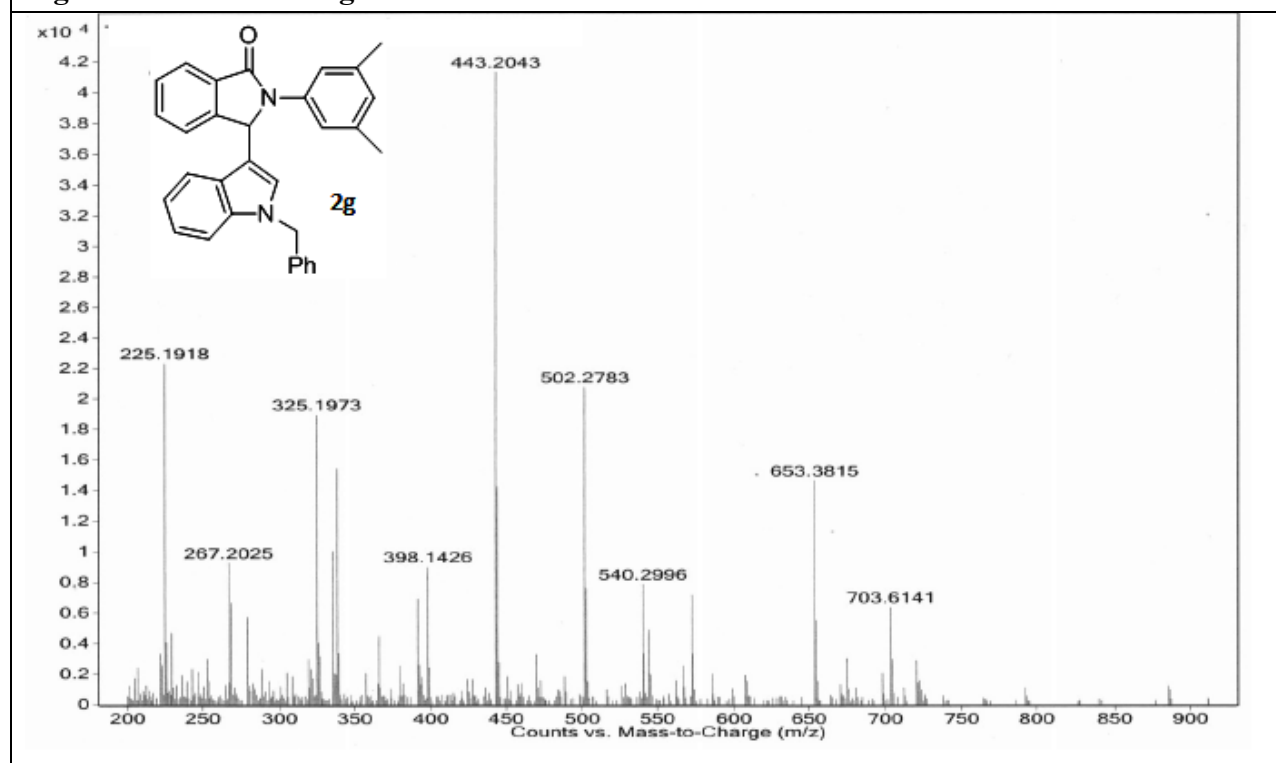


Figure S26. HRMS of **2e**



**Figure S27.** HRMS of **2g**



**Figure S28.** HRMS of **2k**

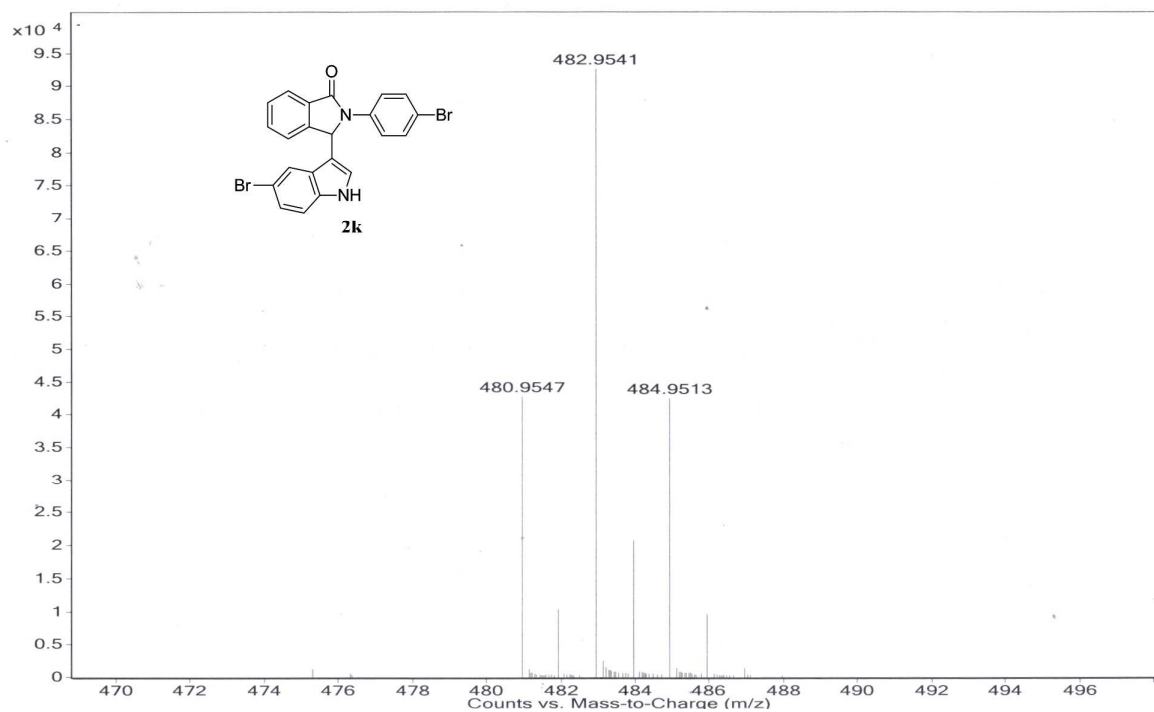


**Figure S29.** HRMS of **2s**

